Journal of Hydrology 590 (2020) 125394

Contents lists available at ScienceDirect

Journal of Hydrology

journal homepage: www.elsevier.com/locate/jhydrol

Research papers

Quantifying future drought change and associated uncertainty in southeastern Australia with multiple potential evapotranspiration models

Lijie Shi[a,b], Puyu Feng[b,c], Bin Wang[b,c,*], De Li Liu[b,d,*], Qiang Yu[c,a,e,*]

[a] School of Life Sciences, Faculty of Science, University of Technology Sydney, PO Box 123, Broadway, Sydney, NSW 2007, Australia
[b] NSW Department of Primary Industries, Wagga Wagga Agricultural Institute, Wagga Wagga, NSW 2650, Australia
[c] State Key Laboratory of Soil Erosion and Dryland Farming on the Loess Plateau, Northwest A&F University, Yangling, Shaanxi 712100, China
[d] Climate Change Research Centre and ARC Centre of Excellence for Climate System Science, University of New South Wales, Sydney, NSW 2052, Australia
[e] College of Resources and Environment, University of Chinese Academy of Science, Beijing 100049, China

ARTICLE INFO

This manuscript was handled by Corrado Corradini, Editor-in-Chief, with the assistance of Juan V. Giraldez, Associate Editor

Keywords:
Standardized precipitation evapotranspiration index
Drought projection
Climate change
Potential evapotranspiration model
Uncertainty

ABSTRACT

Projection of drought under a changing climate is important for drought risk assessment. Changes in precipitation (P) and potential evapotranspiration (ETp) are expected to influence future drought occurrence. Thus, it is important to include both factors to accurately quantify change in drought frequency under future climate scenarios. Standardized precipitation evapotranspiration index (SPEI) is a widely used index in drought assessment because it considers the influence of both P and ETp on drought. Thus, in this study we used SPEI to quantify change in drought frequency under two different emission scenarios (RCP4.5 and RCP8.5) in the wheat belt of southeastern Australia with climatic data downscaled from 34 global climate models (GCMs). We also investigated whether differences ETp models would make a difference on drought projection. Therefore, we employed five different traditional ETp models (Penman, Jensen-Haise, Makkink, Abtew, Hargreaves) and three random forest (RF)-based models to calculate SPEI in this study. Results showed that drought, especially moderate and severe drought, would occur more frequently under future climate scenarios and the increased frequency was generally greater in spring and winter than in summer and autumn. Severe drought occurring in spring would increase by 3.1%–21.7% under RCP4.5 and 5.2%–41.0% under RCP8.5. In autumn, the likely mean increase of severe drought frequency was 0.7%–13.0% under RCP4.5 and 2.7%–27.9% under RCP8.5. Differences in the projected increase of drought frequency were found among the different ETp models. In general, RF-based ETp models, which projected larger increases in ETp, generally also projected larger increases in drought occurrence. A multilinear regression relationship was built between changes in drought frequency and changes in ETp and P. The regression showed that the increased drought frequency was a combined result of the increasing ETp and decreasing P, and that the increasing ETp might be the more dominant factor. The contribution of GCMs, RCPs, different ETp models, and their interaction to the uncertainty in drought projection was quantified with the use of analysis of variance. Results showed that GCMs and their interaction with RCPs were the dominant factors influencing uncertainty in drought projection.

1. Introduction

Drought is a recurring and insidious extreme climate event, which is primarily induced by a prolonged period of deficiency in precipitation (Asadi Zarch et al., 2015). In general, drought can be classified as meteorological (prolonged period of shortage in precipitation), agricultural (insufficient soil moisture to meet crop growth), hydrological (shortage of ground and surface water), or socioeconomic drought (failure of water resource systems to meet demands of people and their activities) (Ayantobo et al., 2017). These droughts can occur in almost all climatic regimes and cause various kinds of damage to human society, such as reduced water supply and crop failure (Asadi Zarch et al., 2015; Mishra and Singh, 2010). For example, the 2006 drought in Australia reduced winter cereal crop production by 36% and resulted in economic loss of AUD$3.5 billion (Wong et al., 2010). Given that increases in air temperature and changes in patterns of precipitation can influence the occurrence of drought events (Mishra and Singh, 2010; Svoboda et al., 2012), it is necessary to project the likely change in

* Corresponding authors at: State Key Laboratory of Soil Erosion and Dryland Farming on the Loess Plateau, Northwest A&F University, Yangling, Shaanxi 712100, China (Q. Yu). NSW Department of Primary Industries, Wagga Wagga Agricultural Institute, Wagga Wagga, NSW 2650, Australia (B. Wang, D.L. Liu).
E-mail addresses: bin.a.wang@dpi.nsw.gov.au (B. Wang), de.li.liu@dpi.nsw.gov.au (D.L. Liu), yuq@nwafu.edu.cn (Q. Yu).

https://doi.org/10.1016/j.jhydrol.2020.125394
Received 27 May 2020; Received in revised form 4 August 2020; Accepted 6 August 2020
Available online 12 August 2020

drought occurrence due to climate change so that agricultural producers and policy makers can take actions to mitigate its dire impacts.

The most common method to study drought change is adopting appropriate drought indices. In general, a drought index is a prime variable derived from one or multiple meteorological or hydrological factors, such as precipitation (P), temperature (T), and potential evapotranspiration (ETp) (Asadi Zarch et al., 2015). It is estimated that more than 160 drought indices have been developed to detect, monitor, and characterize different types of drought (Niemeyer, 2008). Among them, the widely used drought indices include the Rainfall Anomaly Index (RAI), the Standardized Precipitation Index (SPI), the Reclamation Drought Index (RDI), and the Palmer Drought Severity Index (PDSI). Each of these indices has its strengths and weaknesses. For instance, SPI can monitor drought at various timescales, ranging from one month to 72 months (Mckee et al., 1993). However, SPI is based on precipitation alone and fails to consider other variables such as temperature that may also trigger drought events (Svoboda et al., 2012). Thus, SPI may not be suitable for identifying possible changes in drought occurrence and severity under a changing climate, as increasing temperature can have significant effects on drought severity (Vicente-Serrano et al., 2010). In contrast, PDSI is generally cited as a physical index based on soil moisture balance. However, PDSI shows low sensitivity to the variation of ETp because of the standardization procedure of soil water budget anomalies (Cook et al., 2014; Vicente-Serrano et al., 2015), which may make PDSI less suitable under the scenario where ETp changes are considered. In the last decade, the standardized precipitation evapotranspiration index (SPEI), based on the balance between P and ETp (Vicente-Serrano et al., 2010), has been widely used in drought assessment (Potop et al., 2012; Stagge et al., 2015; Vicente-Serrano et al., 2010). Compared with PDSI, SPEI shows equal sensitivity to precipitation and ETp (Vicente-Serrano et al., 2015). Therefore, it might be a better choice for investigating the influence of different ETp models on drought projection. In addition, the multi-scalar characteristics of SPEI enable it to identify different drought types and effects under a changing climate (Vicente-Serrano et al., 2010). Relatively short-term precipitation anomalies generally influence soil moisture conditions, while longer-term precipitation anomalies influence streamflow (Svoboda et al., 2012). Thus, 1- or 2- month SPEI is generally used to assess meteorological drought; anywhere from 1-month to 6-month SPEI is used for agricultural drought (Labudová et al., 2017; Parsons et al., 2019); and any other longer-term SPEI is able to assess hydrological drought (Beguería et al., 2014; Svoboda et al., 2012). The use of 3-month SPEI in seasonal agricultural drought assessment is common in literature (Feng et al., 2018a, 2019; Gao et al., 2017). Feng et al. (2019) combined remotely-sensed factors with 3-month SPEI and found that wheat yields showed high correlation with the 3-month SPEI-assessed drought conditions in southeastern Australia. Based on both 3-month and 12-month SPEI, Yu et al. (2014) assessed changes of drought characteristics from 1951 to 2010 in China and concluded that severe and extreme drought areas have increased by ~3.72% per decade since the 1990s.

Despite the extensive usage of SPEI, there is still controversy regarding which equation should be used to estimate ETp (Beguería et al., 2014; Sheffield et al., 2012; Stagge et al., 2014). Originally, Vicente-Serrano et al. (2010) suggested the use of the Thornthwaite (Th) equation, which only requires monthly mean temperature (Thornthwaite, 1948). However, recent studies have indicated that the Th equation underestimates ETp in arid and semiarid regions and overestimates ETp in humid equatorial and tropical regions (Kumar et al., 1987; Valipour, 2015). Moreover, this equation leads to an overestimation of ETp with increasing air temperature and might not be suitable for climate change studies (Sheffield et al., 2012). Yao et al. (2019) compared the effects of different ETp models on drought assessment based on SPEI in China. They found that the differences of ETp models had greater effects on drought assessment in arid regions than in humid regions. Similarly, Beguería et al. (2014) analyzed the sensitivity of SPEI to three different ETp models and also found that drought assessment was more affected by ETp model choice in arid areas. Thus, selecting an appropriate model to estimate ETp is of great importance for obtaining reliable drought assessment. The physically-based Penman model can normally estimate ETp with high accuracy, but it requires multiple climatic factors as inputs that are sometimes not available. Other empirical models require less input information but are inevitably limited in accuracy. Recently, machine learning methods have gained attention and have shown good performance in ETp estimation (Fan et al., 2018; Shi et al., 2020). For instance, Tabari et al. (2012) developed multiple machine learning methods including support vector machines (SVM), adaptive neuro-fuzzy inference system (ANFIS), multiple linear regression (MLR), and multiple non-linear regression (MNLR) to estimate reference evapotranspiration in Iran. They found that SVM and ANFIS showed better performance than empirical evapotranspiration models when provided with the same input information. However, to the best of our knowledge, there is no study that has been conducted to investigate the influence of ETp estimated by machine learning-based methods on drought assessment with SPEI.

Another problem related to future drought projections is uncertainty (Touma et al., 2015). Climate projections, emission scenarios, and drought indices can all result in uncertainties in drought projections. Quantifying the sources of uncertainty throughout the entire process is crucial for reliable climate change impact assessment (Burke and Brown, 2008; Lu et al., 2019; Taylor et al., 2012). Burke and Brown (2008) projected global changes in drought based on four indices under two different CO_2 scenarios. They found that the increase of areas affected by drought varied from 5% to 45% among different indices, which indicated that there are large uncertainties in future drought projections from drought indices. Similarly, Touma et al. (2015) adopted SPI, the Standardized Runoff Index (SRI), SPEI, and the Supply-Demand Drought Index (SDDI) with data from 15 GCMs to project change in drought under RCP8.5 at global scale. In their study, drought changes projected by SPEI and SDDI were stronger than changes projected by SPI and SRI, demonstrating index-related uncertainty in drought projection. In addition to drought indices, the differences in climate projections, emission scenarios, and ETp models may also result in uncertainty in drought assessment (Aryal et al., 2019; Shi et al., 2020). Lu et al. (2019) projected changes of drought based on soil moisture anomalies using climate data from 17 global climate models (GCMs) and found that the GCMs contributed more than 80% to the uncertainty in the process. However, the contribution of different ETp models to uncertainty in drought projections has rarely been investigated.

The wheat belt in New South Wales (NSW) in southeastern Australia is vulnerable to drought. Under a warming climate, drought is likely to occur more frequently in the future (Feng et al., 2018a, 2019; Kirono et al., 2011; Kirono and Kent, 2011). For instance, based on the 3-month SPEI, Feng et al. (2018a) projected that more frequent and more severe winter-spring droughts were likely to occur in this region, and that these droughts will affect more areas. Similarly, Kirono et al. (2011) adopted RDI with climatic data from 14 GCMs to project drought in Australia and found that more occurrences of drought were likely to happen across NSW in the future. However, these studies generally focused on the projection of future drought without quantifying the uncertainty in their projections. Therefore, not only was our study designed to better understand future changes in drought under different future climate scenarios, but it was also designed to assess the associated uncertainties of future drought projections. An additional objective of our study was to use SPEI driven by different ETp models with climatic data downscaled from multiple GCMs under different emission scenarios (RCPs) to investigate the influence of ETp models on drought projection. Our objective was to answer three questions:

(1) How do different ETp models influence SPEI at different locations in southeastern Australia?

(2) How will drought be changing in the future under different scenarios?
(3) What is the dominant factor determining the uncertainty of future drought projections?

2. Materials and methods

2.1. Study area

The study was designed to assess the effects of climate change on drought in the New South Wales (NSW) wheat belt, in southeastern Australia. Winter wheat (*Triticum aestivum* L.) grown in this region accounts for 28% of the total wheat-planted area in Australia (Feng et al., 2019). However, this region is vulnerable to climate change due to its diverse climate conditions (Wang et al., 2018). In the past decades, wheat yield showed high variation, ranging from 0.62 t ha^{-1} to 2.75 t ha^{-1}, mainly as a result of precipitation variability and drought occurrence (Wang et al., 2015). Therefore, accurate drought projections for this region will be important for predicting both the economy and food supply of NSW.

Temperature in the NSW wheat belt generally increases from the southeast to the northwest while precipitation gradually increases from the southwest to the southeast (Feng et al., 2018a). Gunnedah (31.0°S, 150.3°E) and Wagga Wagga (35.2°S, 147.5°E) are two representative sites in the NSW wheat belt (Fig. 1) that are located in the northeast and southeast, respectively. More importantly, these two sites have long-time series of observed climatic data, including air temperature, solar radiation, relative humidity, precipitation, and wind speed. Both sites experience hot summers and cold winters, but differ in air temperature and annual precipitation. Gunnedah is warmer than Wagga Wagga, with temperature ranging from 12.2 °C to 24.6 °C compared with temperature at Wagga Wagga ranging from 8.9 °C to 22.2 °C. Average annual precipitation values at Gunnedah and Wagga Wagga are 640 mm and 583 mm, respectively. Detailed information for these two sites is shown in Table 1.

2.2. Climatic data

Historical climatic data and future climate scenarios were used to drive ETp models and then for subsequent calculation of the SPEI. For the historical period, observed daily precipitation (P, mm day^{-1}),

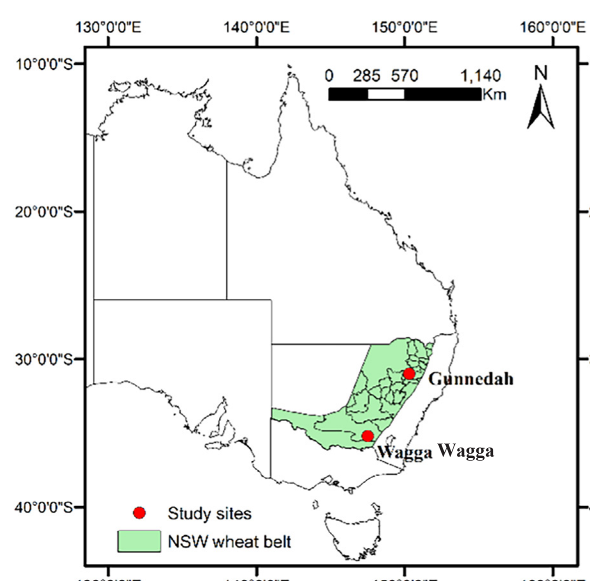

Fig. 1. Location of the two study sites in the wheat belt of New South Wales (NSW), Australia.

maximum and minimum air temperature (T_{max} and T_{min}, °C), maximum and minimum relative humidity (%), and solar radiation (R_s, MJ m^{-2} day^{-1}) at the two sites were obtained from the Scientific Information for Land Owners (SILO) patched point dataset (https://www.longpaddock.qld.gov.au/silo/datadrill/index.php) (Jeffrey et al., 2001). Historical observed daily wind speed (m s^{-1}) at these sites was obtained from the Bureau of Meteorology (BOM, http://www.bom.gov.au/). Climatic data for future climate scenarios was obtained using a statistical downscaling method developed by Liu and Zuo (2012) to extract daily T_{max}, T_{min}, P, and R_s in the period of 1900–2100 from 34 GCMs under the RCP4.5 and RCP8.5 scenarios. A bias correction was conducted to ensure that downscaled GCM climatic data matched well with the historical climatic data (Liu and Zuo, 2012). In this study, we compared the SPEI driven by downscaled GCM data with SPEI driven by observed climate data in the historical period (1971–2010), using a qq-plot technique. Results showed that the simulations with downscaled GCM data matched well with the observations, as shown in Fig. S1 and S2 (Supplementary material). The downscaled data were divided into three periods, namely the baseline period from 1971 to 2010, the near future period from 2021 to 2060 (2040s), and the further future period from 2061 to 2100 (2080s).

2.3. Calculation of potential evapotranspiration

When air temperature, relative humidity, solar radiation, and wind speed are all available, the Penman model is able to accurately estimate ETp (Milly and Dunne, 2016), and has been widely used as a benchmark to estimate performance of other simplified ETp models (Donohue et al., 2010). However, future projections of climatic data downscaled from GCMs, such as wind speed and relative humidity, may not be available or may have low reliability, thereby limiting the use of the Penman model (Guo et al., 2017). In contrast, simplified ETp models such as temperature-based and radiation-based models may have more advantages for future ETp projection because of greater confidence associated with downscaled air temperature than for other climatic data (Randall et al., 2007). In this study, the physically-based Penman model (Penman, 1948), the radiation-based Jensen-Haise (JH), Makkink (Mak), and Abtew (Ab) models, and the temperature-based Hargreaves (HS) model were used to estimate daily ETp. Their mathematical equations are shown in Table 2.

In addition to these traditional ETp models, we also developed machine learning-based ETp models with the use of the random forest (RF) method. RF has been widely used in evapotranspiration estimation (Fan et al., 2018; Feng et al., 2017). One of the advantages of the RF method is that it only requires two parameters to train the model: the number of decision trees (n_{tree}) and the number of variables (m_{try}) (Breiman, 2001). Three RF-based (RF1, RF2, and RF3) ETp models were developed based on different input combinations to compare with the traditional ETp models. RF1 required the same input as JH and Mak (T_{max}, T_{min}, and R_s); RF2 required the same input as HS (T_{max}, T_{min}, and R_a [extra-terrestrial radiation]); and RF3 required the same input as Ab (T_{max} and R_s). The historical climate data (1950/1951–2014) were separated into a set to train the RF models (1950/1951–2000) and a set to test the RF models (2001–2014). In the training process, n_{tree} was set as 500 to guarantee that every input row would be predicted a few times. The value of m_{try} was set as 2 for RF1 and RF2, and 1 for RF3 based on the rule that m_{try} is generally around 1/3 of the number of input variables (Guio Blanco et al., 2018). More information on the development of RF models can be found in Breiman (2001). The "randomForest" package in R (Liaw and Wiener, 2002) (https://cran.r-project.org/web/packages/randomForest/index.html) was used to develop RF-based ETp models in this study.

2.4. Calculation of standardized precipitation evapotranspiration index

The SPEI was developed by Vicente-Serrano et al. (2010) based on a

Table 1
Geographical and long-term averaged meteorological information for Gunnedah and Wagga Wagga, Australia. The geographical information includes longitude (Lon), latitude (Lat), and elevation (DEM). The meteorological information includes air temperature (T), solar radiation (Rs), relative humidity (RH), wind speed (Wind), precipitation (P), and potential evapotranspiration (ETp).

Sites	Lon (degrees)	Lat (degrees)	DEM (m)	T (°C)	Rs (MJ m^{-2} day^{-1})	RH (%)	Wind (m/s)	P (mm $year^{-1}$)	ETp (mm $year^{-1}$)	Period
Gunnedah	150.3	−31.0	307	18.5	18.6	63.2	1.8	640	1650	1951–2014
Wagga Wagga	147.5	−35.2	212	15.5	17.5	67.2	2.0	583	1522	1950–2014

monthly climatic water balance, (i.e., P - ETp), and therefore SPEI accounts for the influence of water demand on drought. In this study, five traditional (Penman, JH, Mak, HS, and Ab) and three machine learning-based (RF1, RF2, and RF3) models were used to estimate daily ETp. The monthly ETp was the accumulation of daily ETp. ETp values estimated from these models were used to calculate SPEI in order to investigate the influence of different ETp models on drought assessment with SPEI. Similar to SPI, SPEI can also be used to assess drought at different time scales (Potop et al., 2012). Three months with P-ETp significantly lower than the normal level will generally result in a decrease in soil moisture, thus leading to crop failure and the occurrence of agricultural drought (Vicente-Serrano et al., 2011). Therefore, a 3-month SPEI can describe soil water conditions during crop growing seasons. In this study, a 3-month time period was used to calculate seasonal SPEI based on the accumulated monthly water balance. For instance, spring SPEI was based on the accumulated water balance from September to November while summer SPEI was based on the accumulated water balance from December to February. Based on the SPEI values, drought was classified as one of three different levels: mild drought ($-1 < \text{SPEI} \leq -0.5$), moderate drought ($-1.5 < \text{SPEI} \leq -1$), and severe drought ($\text{SPEI} \leq -1.5$). Detail information on the calculation of SPEI can be found in Vicente-Serrano et al. (2010).

2.5. Contribution analysis of uncertainty in future drought projection

Differences in GCMs, RCPs, and ETp models can lead to uncertainties in future drought projections. The analysis of variance (ANOVA) technique is capable of partitioning the total observed variances into different sources, thereby identifying the contributions of different sources to the total variance (Aryal et al., 2019). The ANOVA method not only quantifies the relative contributions of different sources to the total variance, but also considers the interactive contributions of different sources of the uncertainty to the total variance (Yip et al., 2011). Therefore, we used a three-way (three factors) ANOVA to quantify the relative and interactive contributions of GCMs, RCPs, and ETp models to the uncertainties in drought projections under future climate scenarios (Morim et al., 2019). A three-way ANOVA can be split into seven fractions that include the three main effects and the four interaction effects. The total sum of squares (SST) was calculated as Eq. (1):

$$SST = SS_{GCMs} + \underbrace{SS_{RCPs}}_{\text{main effects}} + SS_{ETp,models} + SS_{GCMs:RCPs} + SS_{GCMs:ETp,models} + \underbrace{SS_{RCPs:ETp,models}}_{\text{interaction effects}} + SS_{GCMs:RCPs:ETp,models} \quad (1)$$

3. Results

3.1. Droughts occurring in the historical period

Fig. 2 shows the frequency of seasonal drought occurring in the period of 1971–2010 at Gunnedah and Wagga Wagga. Differences in the frequency of mild, moderate, and severe droughts were observed among ETp models. The frequency of mild drought in spring (left columns of upper two panels of Fig. 2) estimated by the Penman model was about 20% at both sites while the other ETp models produced lower frequencies at Gunnedah and higher frequencies at Wagga Wagga. However, the differences in total drought frequency among ETp models were not great (lower two panels of Fig. 2). For instance, the frequency of seasonal drought estimated by the Penman model was generally equal to that estimated by other ETp models at Gunnedah. In addition, mild ($-1 < \text{SPEI} \leq -0.5$) and moderate ($-1.5 < \text{SPEI} \leq -1$) droughts happened more frequently than severe droughts ($\text{SPEI} \leq -1.5$) during the historical period. The average frequency of mild drought at Gunnedah ranged from 9% (in winter) to 20% (in spring) while the corresponding values for severe drought ranged from 2% (in summer) to 6% (in spring).

Differences in ETp estimated by different models are shown in Fig. 3. The RF-based ETp models generally produced similar values as the Penman model. In contrast, the other ETp models generally produced smaller ETp values. However, the underestimated seasonal ETp did not always produce less drought occurrence. This may indicate that drought assessment was mainly dominated by precipitation while ETp

Table 2
Potential evapotranspiration (ETp) models used in this study. The Penman model was used as the benchmark to develop and train the RF-based models and to assess the performance of the RF-based and the empirical ETp models. ETp estimated by the four empirical ETp models was compared with ETp estimated by the RF-based models which required the same inputs. Specifically, JH and Mak were compared with RF1; HS was compared with RF2; and Ab was compared with RF3.

Model	References	Formula	Notes
Penman	Donohue et al. (2010)	$ET_p = \frac{0.408\Delta}{\Delta+\gamma}(R_n - G) + \frac{\gamma}{\Delta+\gamma}\frac{6.43(1+0.536u_2)(e_s-e_a)}{\lambda}$	Open water evaporation, often referred to as Penman potential evaporation
Abtew	Abtew (1996)	$ET_p = 0.01786\frac{R_s T_{\max}}{\lambda}$	ETp from a grass surface
Hargreaves	Hargreaves et al. (1985)	$ET_p = 0.0023 \times 0.408R_a(T_{\max} - T_{\min})^{0.5}(T + 17.8)$	ETp from a grass surface
Jensen-Haise	Jensen and Haise (1963)	$ET_p = 0.0102(T+3)R_s$	ETp from an alfalfa surface
Modified Makkink	Hansen (1984)	$ETp = 0.7\frac{\Delta}{\Delta+\gamma}\frac{R_s}{\lambda}$	ETp from a grass surface

Note: Δ (kPa $°C^{-1}$): the slope of the saturation vapor pressure curve; γ (kPa $°C^{-1}$): the psychrometric constant; R_n (MJ m^{-2} day^{-1}): net radiation; G (MJ m^{-2} day^{-1}): soil heat flux density, assumed to equal to zero for periods of a day or longer (Allen et al., 1998); u_2 (m s^{-1}): wind speed at 2 m height; e_s (kpa): saturation vapor pressure; e_a (kpa): actual vapor pressure; λ (MJ kg^{-1}): the latent heat of vaporization of water, equal to 2.45 MJ kg^{-1} at 20 °C; T_{max} (°C): maximum air temperature; T_{min} (°C): minimum air temperature; T (°C): air temperature; R_s (MJ m^{-2} day^{-1}): solar radiation; R_a (MJ m^{-2} day^{-1}): extra-terrestrial radiation.

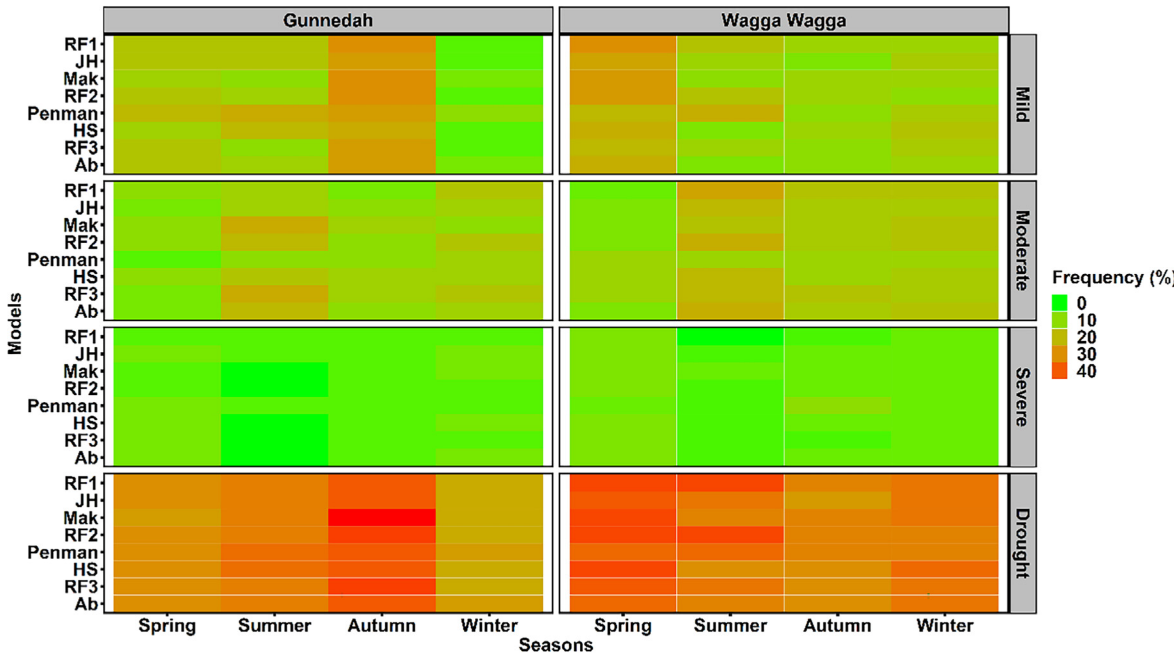

Fig. 2. Frequency of seasonal droughts occurring in the period from 1971 to 2010 at Gunnedah and Wagga Wagga, Australia, using eight potential evapotranspiration models. RF1, RF2, and RF3 (random forest models 1, 2, and 3, respectively); JH (Jensen-Haise); Mak (Makkink); HS (Hargreaves); Ab (Abtew). Mild, moderate, and severe drought classifications are based on standardized precipitation evapotranspiration index values as described in Section 2.3 of the paper. Drought refers to the total of all drought classifications.

played only a minor role in the historical period.

3.2. Projected changes of climatic factors under future scenarios

Minimum (T_{min}) and maximum (T_{max}) air temperatures were all expected to increase under future climate scenarios (Fig. 4, upper panels, a1, a2 and b1, b2). The magnitudes of temperature increases were different in different seasons. Larger mean increases of both T_{min} and T_{max} were generally found in spring and winter. Moreover, the increases in temperature were larger in the 2080s than in the 2040s. By the 2080s (2061–2100), T_{max} was likely to increase by 1.72 °C to 2.33 °C under RCP4.5 and by 3.22 °C to 4.08 °C under RCP8.5. The corresponding increases of T_{min} ranged from 1.73 °C to 2.48 °C under RCP4.5 and from 3.26 °C to 4.64 °C under RCP8.5. Similar to the temperature increases, solar radiation (R_s) was also projected to increase (Fig. 4, lower left panels, c1 and c2) and the R_s increases in the

Fig. 3. Mean seasonal potential evapotranspiration (ETp, mm year^{-1}) from 1971 to 2010 at Gunnedah and Wagga Wagga, Australia calculated by eight ETp models. RF1, RF2, and RF3 (random forest models 1, 2, and 3, respectively); JH (Jensen-Haise); Mak (Makkink); HS (Hargreaves); Ab (Abtew).

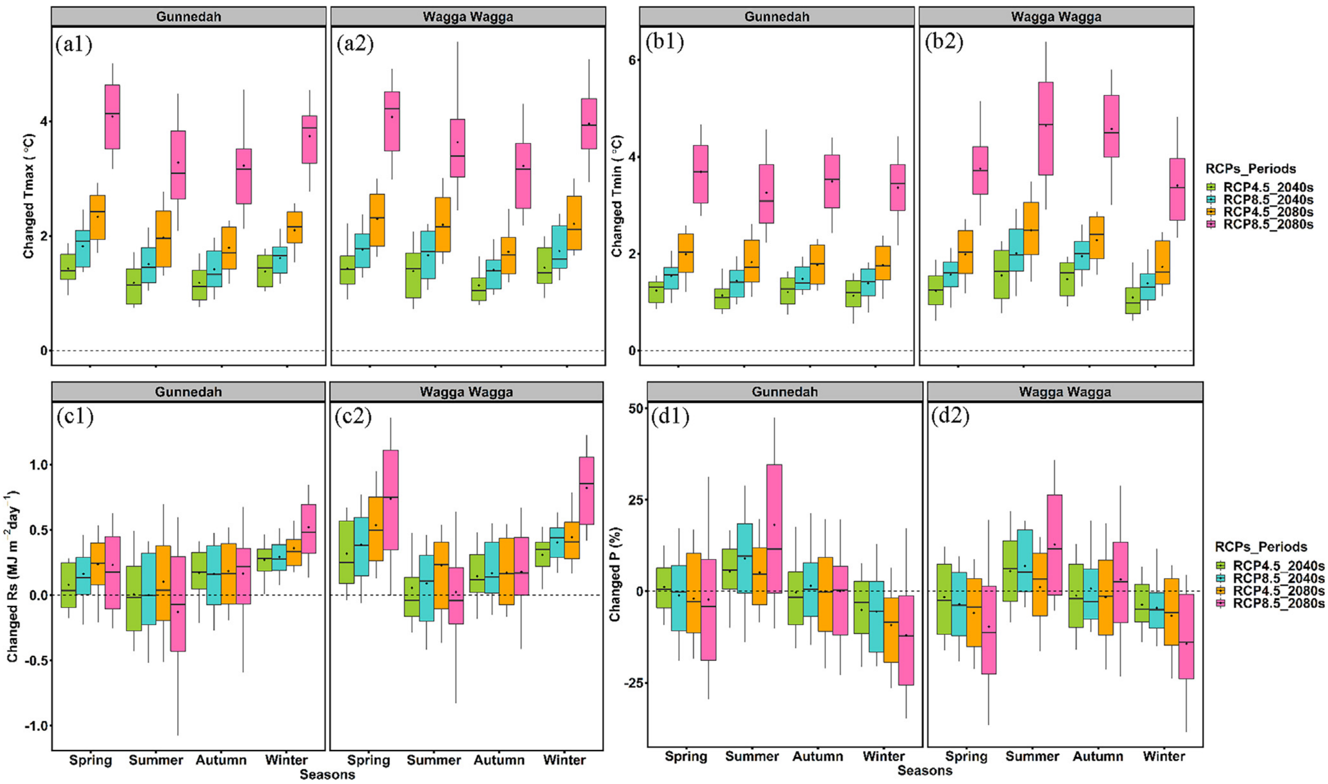

Fig. 4. Projected changes in maximum (Tmax, °C, a1, a2) and minimum (Tmin, °C, b1, b2) air temperature, solar radiation (Rs, MJ m^{-2} day^{-1}, c1, c2), and precipitation (P, %, d1, d2) in the 2040s and 2080s at Gunnedah (a1, b1, c1, d1) and Wagga Wagga (a2, b2, c2, d2), Australia, under RCP4.5 and RCP8.5 scenarios. Lower and upper box boundaries indicate the 25th and 75th percentiles, respectively. The black line and dot inside each box indicate the median and mean, respectively. The lower and upper whiskers indicate the 10th and 90th percentiles, respectively.

further future period were larger. Regarding seasonal variation, R_s in winter showed the largest mean increases followed by the increases in spring and autumn R_s, which were generally close. The increases in R_s during winter by the 2080s were 0.36 MJ m^{-2} day^{-1} at Gunnedah and 0.44 MJ m^{-2} day^{-1} at Wagga Wagga under RCP4.5, and 0.52 MJ m^{-2} day^{-1} at Gunnedah and 0.82 MJ m^{-2} day^{-1} at Wagga Wagga under RCP8.5.

The projected changes in P showed seasonal variation under future climate scenarios (Fig. 4, lower right panels, d1 and d2). Specifically, summer P was projected to increase at both sites. The mean increase of summer P ranged from 1.14% to 5.49% under RCP4.5 and ranged from 6.93% to 18.10% under RCP8.5. In contrast, spring and winter P was likely to decrease. The maximum mean decreases of spring and winter P were 9.72% and 14.34%, respectively. Even though the predicted autumn P in the future was observed to be similarly variable as predicted for other seasons, the mean values of autumn P under future scenarios were close to those in the baseline period.

3.3. Projected changes of potential evapotranspiration under future climate scenarios

ETp projected by all models was likely to increase under future climate scenarios, although the magnitudes of increase varied among models (Fig. 5). In general, RF-based models (followed by JH and Ab) produced larger ETp increases, whereas Mak and HS yielded smaller increases. Moreover, the ETp increases showed similar seasonal variation with that of temperatures, i.e., larger increases were generally observed in spring and winter, whereas smaller increases were observed in summer and autumn. By the 2080s (2061–2100), the mean increases in spring ETp ranged from 4.6% to 15.6% under RCP4.5 and from 7.7% to 26.9% under RCP8.5; the mean summer ETp values were likely to increase by 2.9% to 10.1% under RCP4.5 and by 3.5% to 16.1% under RCP8.5; in autumn, the projected increase of mean ETp ranged from 2.9% to 11.2% under RCP4.5 and from 3.6% to 22.7% under RCP8.5; and the likely increases in mean winter ETp ranged from 7.5% to 23.3% and 13.1% to 44.0% under RCP4.5 and RCP8.5, respectively. Results of the multiple linear regression (Fig. 6, ΔETp (%) = a_0 * ΔT_{max} (°C) + b_0 * ΔT_{min} (°C) + c_0 * ΔR_s (MJ m^{-2} day^{-1})) showed that changes in ETp could be almost entirely explained by changes in T_{max}, T_{min}, and R_s. However, the sensitivity of ETp models to these climatic factors varied. In general, models requiring the same inputs showed similar sensitivity to the same climatic factors. For instance, ETp estimated by RF1, JH, and Mak was more sensitive to changes in R_s than to changes in T_{max} or T_{min}. In contrast, a unit increase in T_{max} led to a larger increase in ETp estimated by HS and RF2 than R_s did.

3.4. Projected changes in drought frequency and their relationship with climatic factors

Compared with the baseline period (1971–2010), droughts, especially moderate (Fig. 7, upper right panels) and severe (Fig. 7, lower left panels) droughts, were projected to occur more frequently in the future (Fig. 7 and Fig. S3). The amount of increase projected by different ETp models was different. Compared with traditional ETp models, RF-based models generally produced larger increases than traditional ETp models, except for JH which projected similar or even larger increases. For example, RF1 projected that summer severe drought would increase by 28.4% on average by the 2080s under RCP8.5 at Wagga Wagga while the corresponding increase projected by Mak was 5.7%. In addition, the increase of drought frequency under RCP8.5 was larger than that observed under RCP4.5. Severe drought occurring in spring would increase by 3.1% to 21.7% under RCP4.5 and by 5.2% to 41.0% under RCP8.5. Frequency of winter severe drought was likely to increase by 4.5% to 20.9% under RCP4.5 and by 7.9% to 37.4% under RCP8.5. The

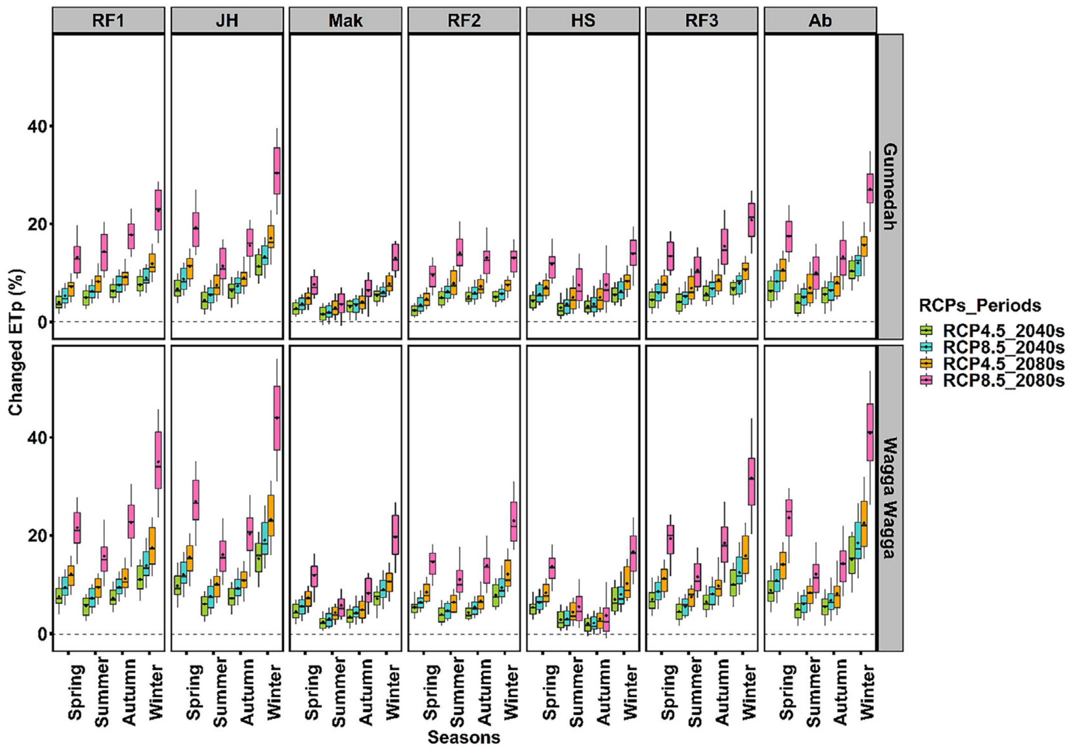

Fig. 5. Projected changes in potential evapotranspiration (ETp, %) in the near future (2021–2060, 2040s) and further future (2061–2100, 2080s) at Gunnedah and Wagga Wagga, Australia, under RCP4.5 and RCP8.5 scenarios based on 34 GCMs compared with baseline values (1971–2010). Lower and upper box boundaries indicate the 25th and 75th percentiles, respectively. The black line and dot inside each box mark the median and mean, respectively. The lower and upper whiskers indicate the 10th and 90th percentiles, respectively.

increased frequency of summer and autumn droughts was smaller than the increased frequency of spring and winter droughts. By the 2080s, the maximum mean increase of summer severe drought would be 18.3% under RCP4.5 and 28.4% under RCP8.5. The corresponding increases for autumn severe drought would be 13.0% under RCP4.5 and 27.9% under RCP8.5.

Changing P pattern and increasing ETp were expected to exert their influence on frequency of drought occurrences under future climate scenarios. To investigate the contribution of changes in climatic factors to drought frequency, multiple linear regression was performed after checking for multicollinearity among independent factors based on the variance inflation factor (VIF). In this study, independent factors with VIF values greater than 10 (Supplementary Table S1) were discarded to minimize the influence of multicollinearity (Feng et al., 2018b). Thus, only ETp and P were retained while T_{min}, T_{max}, and R_s were discarded to build the regression relationship (ΔF (%) = a * ΔP (%) + b * ΔETp (%)) between changes in drought frequency and changes in climatic factors. Fig. 8 shows that changes in P and ETp mainly (generally greater than 80% contribution) explained the change in the frequency of severe drought at both locations. In addition, a unit increase in ETp generally caused a larger increase in drought frequency than caused by a unit decrease in P. For example, the ETp regression coefficient (b) ranged from 1.09 to 1.84 among ETp models for severe drought in spring at Gunnedah (Fig. 8), while the absolute value of the P coefficient (a) ranged from 0.36 to 0.46. The larger absolute values of regression coefficients for ETp compared with P indicated that changes in ETp were the major factor resulting in greater frequency of drought.

3.5. Uncertainty analysis in drought projection

The contributions of different sources of variation and their interactions to the total uncertainty in projecting drought frequency are shown in Fig. 9. GCMs and their interaction with RCPs (GCMs:RCPs) contributed the most to the total uncertainty independent of drought level, season, and site. The uncertainty contribution of GCMs and GCMs:RCPs ranged from 19.2% to 53.0% and from 17.2% to 44.3%, respectively. The contribution of RCPs to severe drought and the interaction of GCMs, RCPs, and ETp models (GCMs:RCPs:Models) to mild and moderate droughts were also large. In contrast, the contribution of ETp models to the total uncertainty was negligible, generally < 5.0%. The results of this uncertainty analysis indicated that the projection of drought under future climate was only slightly influenced by the differences in ETp models, but greatly influenced by GCMs and RCPs.

4. Discussion

This study used SPEI computed from P and ETp estimated by different ETp models to project the potential change in drought occurrence under the RCP4.5 and RCP8.5 climate scenarios for two sites in the wheat belt of southeast Australia. In addition, the sensitivity of SPEI to different ETp models and the contribution of different sources to the uncertainty of drought projection were also analyzed. During the historical period, the total occurrence of drought showed little difference among different ETp models (Fig. 2). However, differences among ETp models could be found in the frequency of mild, moderate, and severe droughts. In contrast, differences in the increase in drought frequency projected by different ETp models was larger during the future period (Fig. 7 and Fig. S3). The differences generally indicated that RF-based models projected larger increases in drought frequency (especially for severe drought) than traditional ETp models did. This pattern was also found in the projection of increases in ETp (Fig. 5), i.e., ETp models which produced larger increases in ETp in the future also projected larger increases in drought frequency in the future. Yao et al. (2019) assessed the influence of different ETp models on drought monitoring in China with the use of SPEI. They concluded that the accuracy of ETp models played only a minor role in drought assessments at wetter sites

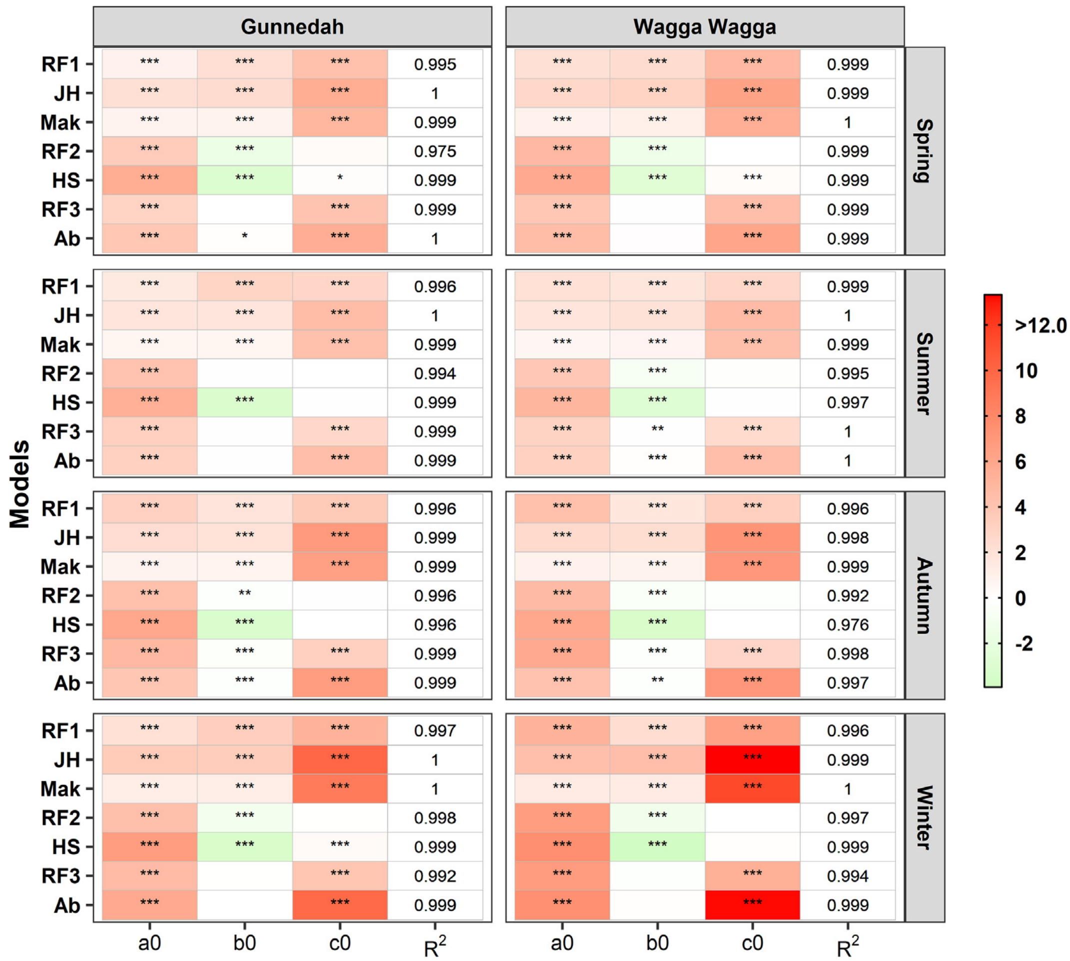

Fig. 6. Regression coefficients for changes in ETp (ΔETp, %) at Gunnedah and Wagga Wagga, southeast Australia, with changes in T_{max} (ΔT_{max}, °C), T_{min} (ΔT_{min}, °C), and R_s (ΔR_s, MJ m^{-2} day^{-1}) in a multiple liner regression model (ΔETp (%) = $a_0 * \Delta T_{max}$ (°C) + $b_0 * \Delta T_{min}$ (°C) + $c_0 * \Delta R_s$ (MJ m^{-2} day^{-1})) for seven ETp models; ***:p < 0.001, **:p < 0.01; *:p < 0.05. RF1, RF2, and RF3 (random forest models 1, 2, and 3, respectively); JH (Jensen-Haise); Mak (Makkink); HS (Hargreaves); Ab (Abtew). Units for a_0 and b_0 are % $°C^{-1}$; units for c_0 are % (MJ m^{-2} $day^{-1})^{-1}$. The color legend represents the values of a_0, b_0, and c_0.

where P was greater than 500 mm $year^{-1}$, while ETp models made a large difference in drought assessment at drier sites. The mean historical annual P at our study sites was slightly greater than 500 mm, but it was projected to decrease (Fig. 4, d1 and d2) under future climate scenarios. This can explain why the influence of different ETp models on drought projection was greater in the future periods. Additionally, other studies (Asadi Zarch et al., 2017, 2015; Cook et al., 2014) have shown that ETp was more important to future drought projection than to historical drought assessment. For instance, Asadi Zarch et al. (2015) used both SPI (based only on P) and RDI (based on ETp and P) to assess changes in global drought. They found that there was a significant agreement in drought assessment between SPI and RDI only in historical periods. However, a significant difference was observed in future drought projection between the two methods, and RDI projected more occurrences of drought in the future than SPI did. They stated that "agreement between SPI and RDI is affected and decreases remarkably over time". Therefore, it is necessary to include ETp in future drought projection studies and attention should also be given to ETp model use.

Increases in drought frequency at Wagga Wagga were generally larger than those observed at Gunnedah (Fig. 7). This may be explained by the greater increases in temperature and solar radiation at Wagga Wagga. Additionally, precipitation is likely to be somewhat less at Wagga Wagga than at Gunnedah in the future (Fig. 4, d1 and d2). During the historical period, Wagga Wagga was also slightly drier than Gunnedah. Thus, the greater increase in drought is likely to present greater challenges to agricultural production at this site. In addition to the increase in future drought projected by offline indices, direct GCM outputs, such as soil moisture and runoff, have also supported the increase in future drought on a large scale (Zhang et al., 2018; Zhao and Dai, 2015, 2017). For instance, Zhao and Dai (2015) used sc_PDSI, soil moisture in the 0–10 cm surface soil layer, and runoff from 14 GCMs to project drought under the RCP4.5 scenario at global scale. They found that all of these measures projected increases in drought over most land areas. Although general increases have been widely reported across the world, the magnitudes of the increases have varied among studies (Dai, 2013; Dai and Zhao, 2017; Milly and Dunne, 2016; Naumann et al., 2018). Based on 12-month SPEI with the Penman-Monteith model, Naumann et al. (2018) projected that drought magnitudes could double for 30% of the global landmass with 1.5 °C warming. Meanwhile, they found that water supply–demand deficit could increase by fivefold for Australia if contemporary warming rates continue. However, Milly and Dunne (2016) reported that ETp-dependent metrics may overpredict drought increases. Similarly, Yang et al. (2018) found that regardless of the obvious drying atmosphere trend for the 21st century, surface runoff was likely to increase across most of the global land area. In our study, the increases in drought varied greatly depending on seasons, ETp models, and climate scenarios (Fig. 7). The discrepancies among these studies demonstrate the need for further research studies in drought projection. The discrepancies also indicate that drought projection is partially influenced by drought definition and the indices used. The results of our study provide a substantial contribution to the debate on the effect of different ETp models on drought quantification.

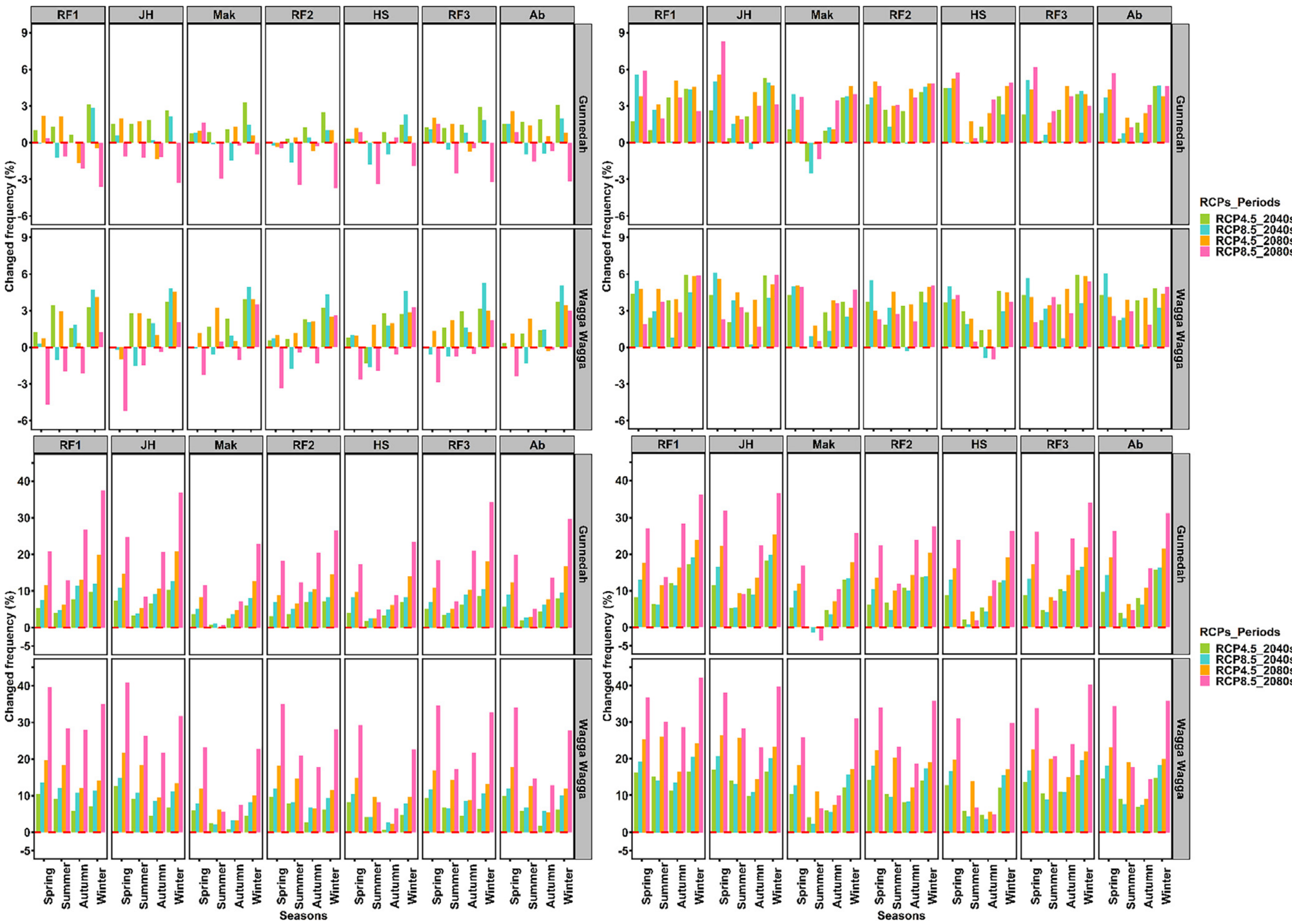

Fig. 7. Changes in the frequency of seasonal mild drought (upper left panels, $-1 < \text{SPEI} \leq -0.5$), moderate drought (upper right panels, $-1.5 < \text{SPEI} \leq -1$), severe drought (lower left panels, $\text{SPEI} \leq -1.5$), and the total drought ($\text{SPEI} \leq -0.5$) in the near (2021–2060, 2040s) and further (2061–2100, 2080s) future periods compared with the baseline period (1971–2100) at Gunnedah and Wagga Wagga, Australia. The calculation of SPEI was based on seven ETp models driven by downscaled climatic data from 34 GCMs under RCP4.5 and RCP8.5 scenarios. Data presented are changed mean frequency in the 40-year values for the 34 GCMs compared with that of the baseline period. RF1, RF2, and RF3 (random forest models 1, 2, and 3, respectively); JH (Jensen-Haise); Mak (Makkink); HS (Hargreaves); Ab (Abtew).

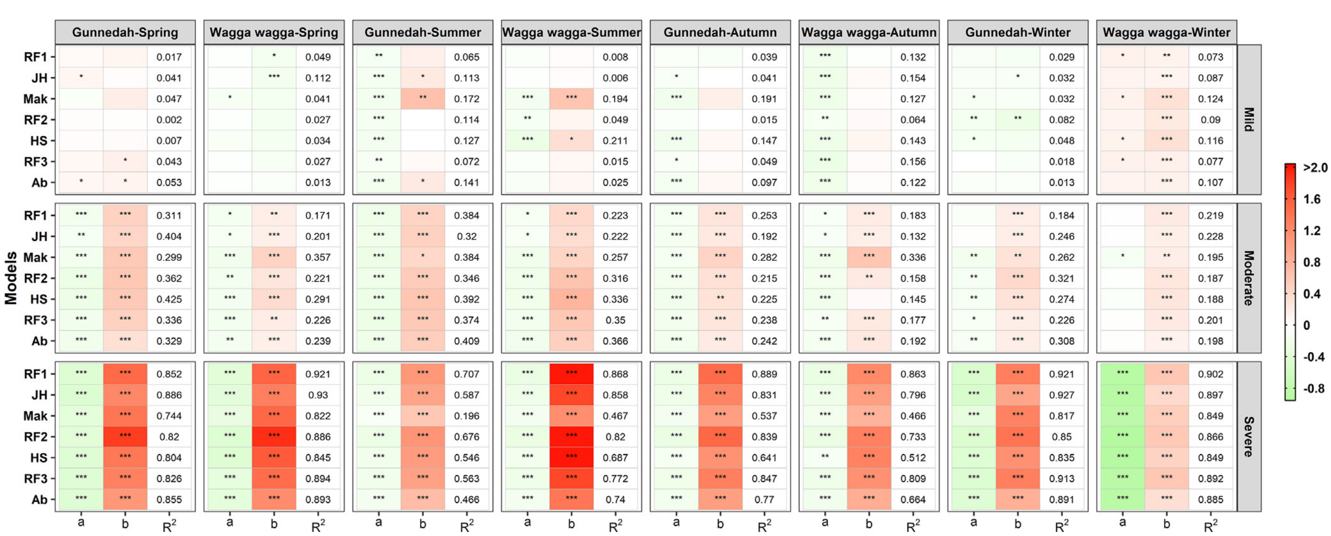

Fig. 8. Regression coefficients for changes in frequency of seasonal droughts (ΔF, %) at Gunnedah and Wagga Wagga, Australia with changes in precipitation (ΔP, %) and potential evapotranspiration (ΔETp, %) in a multiple liner regression model ($\Delta F\ (\%) = a * \Delta P\ (\%) + b * \Delta ETp\ (\%)$) for seven ETp models; ***:$p < 0.001$, **:$p < 0.01$; *:$p < 0.05$. RF1, RF2, and RF3 (random forest models 1, 2, and 3, respectively); JH (Jensen-Haise); Mak (Makkink); HS (Hargreaves); Ab (Abtew). Coefficients a and b are dimensionless. The color legend represents the values of a and b.

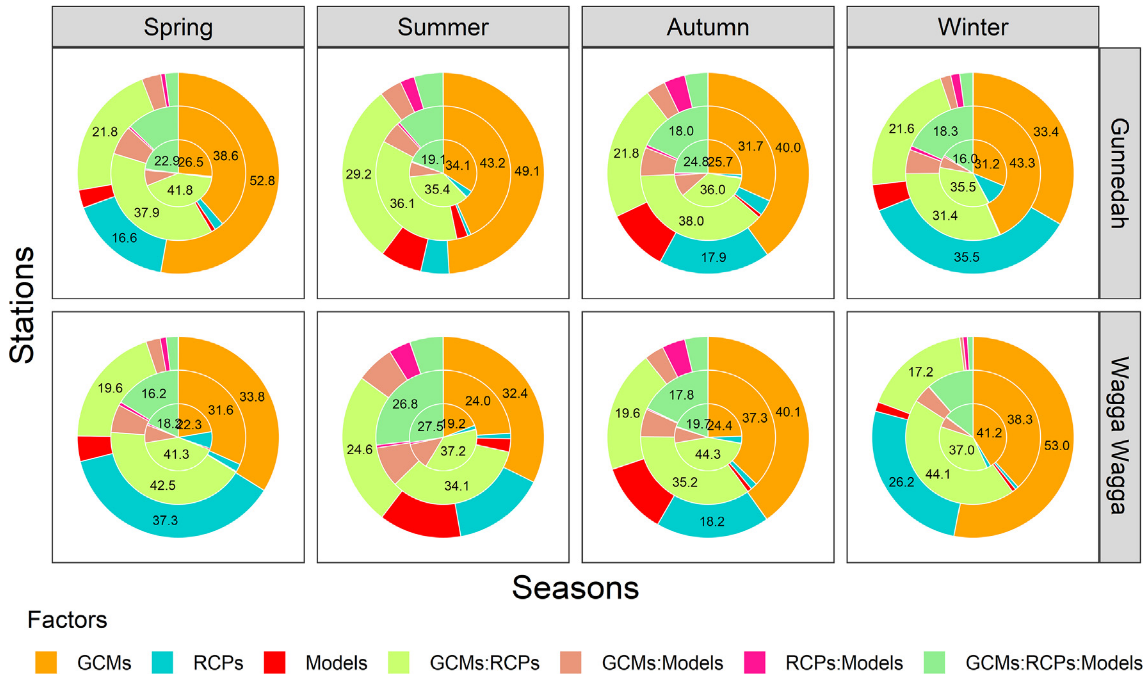

Fig. 9. Contribution (%) of GCMs, RCPs, and ETp models to the uncertainty in drought frequency projection at Gunnedah and Wagga Wagga, Australia for each season. Results for mild, moderate, and severe drought are shown from inward to outward circles, respectively. Contributions larger than 15% are shown by numbers in the figure.

According to our study, more frequent and severe drought under future climate scenarios was generally the result of a combined effect of increasing ETp and decreasing P (Fig. 8) and the increase of ETp might play a major role in the increase of drought in the future period. Similar to our study, Cook et al. (2014) also found that declines in P would push the climate towards drought while the increased ETp would amplify the precipitation-induced drought. The projected increase in drought occurrence will inevitably lead to decreased crop yields and cause more challenges to cropping systems (van Dijk et al., 2013; Lobell et al., 2015). Because spring and winter are key growing seasons for wheat and canola (*Brassica napus* L.) in this region of Australia and because these crops are mainly grown under rainfed conditions, they will be more vulnerable to drought-induced yield losses in the future (Feng et al., 2020; Luo et al., 2005). Thus, measures should be taken to minimize the negative influence of droughts. Breeding new crop varieties that have greater drought tolerance, use of irrigation, and changing planting date are three possible measures that could mitigate drought-induced yield loss (Chenu et al., 2011; Watson et al., 2017).

This study found that differences in GCMs and their interaction with RCPs (GCMs:RCPs) contributed the most to the uncertainty in the process of drought projection (19.2%–53% and 17.2%–44.3%, respectively; Fig. 9). Lu et al. (2019) found that differences in GCMs could account for more than 80% of the uncertainty in drought projection based on soil moisture anomalies. The large contribution of GCMs might be due to the differences in P projected by different GCMs. For instance, Hawkins and Sutton (2011) found that GCMs generally played a dominant role among GCMs, RCPs, and the random, internal variations in climate with regard to the uncertainty of P projection for lead times longer than 30 years. Different RCPs generally resulted in different temperature predictions, which would influence ETp prediction. Shi et al. (2020) found that RCP differences could explain around 40% of the uncertainty in ETp projection. This may explain why the GCMs:RCPs interaction also played a key role in the uncertainty of drought projection in our study. The dominant contribution of GCMs and GCMs:RCPs to drought assessment highlighted the importance of using a wide range of GCMs and different emission scenarios to avoid the underestimation of the total uncertainty. For policymakers, the less uncertainty that there is in drought projections, the more reliable are the measures that can be recommended. Therefore, the possibility of reducing uncertainty in drought projection should be investigated in the future. The availability of more and more GCMs from CMIP6 might provide the possibility of reducing such uncertainty through the consideration of more environmental factors, the use of more advanced numerical simulation methods, and the generally higher resolution (Eyring et al., 2016).

A few limitations in our study should be acknowledged. In addition to SPEI, there are other drought indices such as RDI (Tsakiris et al., 2007), and their sensitivity to different ETp models was not reported in this study. Therefore, more drought indices should be included in future studies to better understand the comprehensive influence of evapotranspiration on drought. In addition, the influence of enriched CO_2 environment on drought projection is complex (Berdugo et al., 2020; Vicente-Serrano et al., 2020). There were two reasons for why we did not consider CO_2 fertilization in our study. First, we used the open-water Penman model rather than the reference crop Penman-Monteith model to calculate ETp instead of ET0 or actual evapotranspiration. Second, increasing atmospheric CO_2 concentration is expected to influence plant structure (e.g., leaf size, root length), and function (e.g., stomatal resistance, vegetation evapotranspiration) (Pritchard et al., 1999; Yang et al., 2019). Thus, the effects of enriched CO_2 on drought projection should ideally involve a consideration of other biophysical factors such as plant development and their response to the changing meteorological factors (Sheffield et al., 2012). The biophysical modelling component was not considered in our study. Recently, Yang et al. (2019) modified the Penman-Monteith model by adding a trained relationship between CO_2 and surface resistance to consider the influence of elevated CO_2 on ET0. They adopted the modified and the original Penman-Monteith model, and direct outputs from 16 GCMs to project global drought under RCP8.5 based on PDSI, and observed that the degree of increase in drought was much smaller with the modified Penman-Monteith model because the elevated CO_2 offset the ET0 increase caused by increased temperature (Yang et al., 2020). Their study sets an example for future studies to comprehensively assess the influence of climate change on drought with consideration of plant response to elevated CO_2. However, elevated CO_2 will not only lead to partial stomatal closure (reducing evapotranspiration) but will also lead to larger leaf size (Pritchard et al., 1999) (increasing evapotranspiration). Additionally, as Berdugo et al. (2020) reported in their response to Keenan et al. (2020), the positive effect of CO_2 fertilization on vegetation growth and evapotranspiration may be dampened or even reversed by the effects of increased soil temperature, continued drying, and extreme climatic events in the future. In this context, there is a need to consider other important factors when exploring the impacts of climate change and CO_2 fertilization on future drought.

5. Conclusions

This study used SPEI to project possible changes of drought under two different emission scenarios (RCP4.5 and RCP8.5) for two locations in the wheat belt of southeastern Australia based on climate data downscaled from 34 GCMs. Three newly developed random forest (RF1, RF2, and RF3) models and five traditional potential evapotranspiration (ETp) models were used to calculate SPEI to investigate the influence of ETp models on drought assessment. The influence of ETp models on drought assessment with SPEI was evident for future periods even though little difference was observed among these ETp models in the historical drought assessment period. Generally, RF-based ETp models which projected larger increases in ETp also projected larger increases in drought frequency. This finding emphasized the necessity of using drought indices which include both P and ETp to predict drought under a changing climate. A greater increase in frequency of moderate and severe droughts was predicted than for mild droughts. The increased occurrence of droughts showed seasonal variations, with larger increases in spring and winter and smaller increases in autumn and winter. For instance, the maximum mean increase of frequency of severe drought in spring was 21.7% under RCP4.5 and 41.0% under RCP8.5 by the 2080s, while the corresponding increase for autumn severe drought was 13.0% under RCP4.5 and 27.9% under RCP8.5. The projection of droughts under future climate scenarios was accompanied by uncertainties. Our study showed that the uncertainty was mainly due to differences in GCMs (19.2%–53%) followed by the interaction of GCMs with RCPs. Despite the uncertainty, results from our study highlight the necessity of identifying mitigation and adaptation strategies to deal with the potential negative impacts caused by more moderate and severe droughts in the future.

Credit authorship contribution statement

Lijie Shi: Conceptualization, Formal analysis, Investigation, Methodology, Visualization, Writing - original draft. **Puyu Feng:** Software, Visualization, Writing - review & editing. **Bin Wang:** Methodology, Supervision, Writing - review & editing. **De Li Liu:** Supervision, Data curation, Writing - review & editing. **Qiang Yu:** Funding acquisition, Project administration, Supervision, Writing - review & editing.

Declaration of Competing Interest

The authors declare that they have no known competing financial interests or personal relationships that could have appeared to influence the work reported in this paper.

Acknowledgements

The first author acknowledges the China Scholarship Council (201706300020) and University of Technology Sydney (12818579) for a scholarship and the Wagga Wagga Agricultural Institute for providing office facilities to carry out this work. This research was also supported by Natural Science Foundation of China (41961124006, 41730645).

We thank the Scientific Information for Land Owners and the Bureau of Meteorology for offerings the climatic data used in this work. We also appreciate the Program for Climate Model Diagnosis and Intercomparison and the WCRP's Working Group on Coupled Modelling for their contribution in the achievement of the WCRP CMIP5 GCMs dataset.

Appendix A. Supplementary data

Supplementary data to this article can be found online at https://doi.org/10.1016/j.jhydrol.2020.125394.

References

Abtew, W., 1996. Evapotranspiration measurements and modeling for three wetland systems in south Florida. J. Am. Water Resour. Assoc. 32 (3), 465–473.
Allen, R.G., Pereira, L.S., Raes, D., Smith, M., 1998. Crop evapotranspiration – guidelines for computing Crop Water Requirements. FAO Irrigation & Drainage Paper 56, Rome, Italy.
Aryal, A., Shrestha, S., Babel, M.S., 2019. Quantifying the sources of uncertainty in an ensemble of hydrological climate-impact projections. Theor. Appl. Climatol. 135 (1), 193–209. https://doi.org/10.1007/s00704-017-2359-3.
Asadi Zarch, M.A., Sivakumar, B., Sharma, A., 2015. Droughts in a warming climate: a global assessment of Standardized precipitation index (SPI) and Reconnaissance drought index (RDI). J. Hydrol. 526, 183–195. https://doi.org/10.1016/j.jhydrol.2014.09.071.
Asadi Zarch, M.A., Sivakumar, B., Malekinezhad, H., Sharma, A., 2017. Future aridity under conditions of global climate change. J. Hydrol. 554, 451–469. https://doi.org/10.1016/j.jhydrol.2017.08.043.
Ayantobo, O.O., Li, Y.i., Song, S., Yao, N., 2017. Spatial comparability of drought characteristics and related return periods in mainland China over 1961–2013. J. Hydrol. 550, 549–567. https://doi.org/10.1016/j.jhydrol.2017.05.019.
Beguería, S., Vicente-Serrano, S.M., Reig, F., Latorre, B., 2014. Standardized precipitation evapotranspiration index (SPEI) revisited: parameter fitting, evapotranspiration models, tools, datasets and drought monitoring. Int. J. Climatol. 34 (10), 3001–3023. https://doi.org/10.1002/joc.3887.
Berdugo, M., Soliveres, S., Delgado-Baquerizo, M., Maestre, F.T., 2020. Ecosystem aridity and atmospheric CO2 —response. Science 368 (6488), 252. https://doi.org/10.1126/science.abb5840.
Breiman, L., 2001. Random Forests. Mach. Learn. 45 (1), 5–32. https://doi.org/10.1023/A:1010933404324.
Burke, E.J., Brown, S.J., 2008. Evaluating uncertainties in the projection of future drought. J. Hydrometeorol. 9 (2), 292–299. https://doi.org/10.1175/2007jhm929.1.
Chenu, K., et al., 2011. Environment characterization as an aid to wheat improvement: interpreting genotype-environment interactions by modelling water-deficit patterns in North-Eastern Australia. J. Exp. Bot. 62 (6), 1743–1745. https://doi.org/10.1093/jxb/erq459.
Cook, B.I., Smerdon, J.E., Seager, R., Coats, S., 2014. Global warming and 21st century drying. Clim. Dyn. 43 (9), 2607–2627. https://doi.org/10.1007/s00382-014-2075-y.
Dai, A., 2012. Increasing drought under global warming in observations and models. Nat. Clim. Change 3, 52. https://doi.org/10.1038/nclimate1633.
Dai, A., Zhao, T., 2017. Uncertainties in historical changes and future projections of drought. Part I: estimates of historical drought changes. Clim. Change 144 (3), 519–533. https://doi.org/10.1007/s10584-016-1705-2.
Donohue, R.J., McVicar, T.R., Roderick, M.L., 2010. Assessing the ability of potential evaporation formulations to capture the dynamics in evaporative demand within a changing climate. J. Hydrol. 386 (1-4), 186–197. https://doi.org/10.1016/j.jhydrol.2010.03.020.
Eyring, V., et al., 2016. Overview of the Coupled Model Intercomparison Project Phase 6 (CMIP6) experimental design and organization. Geoscientific Model Dev. 9 (5), 1937–1958. https://doi.org/10.5194/gmd-9-1937-2016.
Fan, J., Yue, W., Wu, L., Zhang, F., Cai, H., Wang, X., Lu, X., Xiang, Y., 2018. Evaluation of SVM, ELM and four tree-based ensemble models for predicting daily reference evapotranspiration using limited meteorological data in different climates of China. Agric. For. Meteorol. 263, 225–241. https://doi.org/10.1016/j.agrformet.2018.08.019.
Feng, Y.u., Cui, N., Gong, D., Zhang, Q., Zhao, L.u., 2017. Evaluation of random forests and generalized regression neural networks for daily reference evapotranspiration modelling. Agric. Water Manage. 193, 163–173. https://doi.org/10.1016/j.agwat.2017.08.003.
Feng, P., Liu, D.L., Wang, B., Waters, C., Zhang, M., Yu, Q., 2018a. Projected changes in drought across the wheat belt of southeastern Australia using a downscaled climate ensemble. Int. J. Climatol. 39 (2), 1041–1053. https://doi.org/10.1002/joc.5861.
Feng, P., Wang, B., Liu, D.L., Xing, H., Ji, F., Macadam, I., Ruan, H., Yu, Q., 2018b. Impacts of rainfall extremes on wheat yield in semi-arid cropping systems in eastern Australia. Clim. Change 147 (3), 555–569. https://doi.org/10.1007/s10584-018-2170-x.
Feng, P., Wang, B., Liu, D.L., Yu, Q., 2019. Machine learning-based integration of remotely-sensed drought factors can improve the estimation of agricultural drought in South-Eastern Australia. Agric. Syst. 173, 303–316. https://doi.org/10.1016/j.agsy.2019.03.015.

Feng, P., Wang, B., Luo, J.-J., Liu, D.L., Waters, C., Ji, F., Ruan, H., Xiao, D., Shi, L., Yu, Q., 2020. Using large-scale climate drivers to forecast meteorological drought condition in growing season across the Australian wheatbelt. Sci. Total Environ. 724, 138162. https://doi.org/10.1016/j.scitotenv.2020.138162.
Gao, X., Zhao, Q.i., Zhao, X., Wu, P., Pan, W., Gao, X., Sun, M., 2017. Temporal and spatial evolution of the standardized precipitation evapotranspiration index (SPEI) in the Loess Plateau under climate change from 2001 to 2050. Sci. Total Environ. 595, 191–200. https://doi.org/10.1016/j.scitotenv.2017.03.226.
Guio Blanco, C.M., Brito Gomez, V.M., Crespo, P., Ließ, M., 2018. Spatial prediction of soil water retention in a Páramo landscape: methodological insight into machine learning using random forest. Geoderma 316, 100–114. https://doi.org/10.1016/j.geoderma.2017.12.002.
Guo, D., Westra, S., Maier, H.R., 2017. Sensitivity of potential evapotranspiration to changes in climate variables for different Australian climatic zones. Hydrol. Earth Syst. Sci. 21 (4), 2107–2126. https://doi.org/10.5194/hess-21-2107-2017.
Hansen, S., 1984. Estimation of Potential and Actual Evapotranspiration. Paper presented at the Nordic Hydrological Conference (Nyborg, Denmark, August – 1984), vol. 15(4-5), pp. 205–212.
Hargreaves, G.L., Hargreaves, G.H., Riley, J.P., 1985. Irrigation water requirements for Senegal River Basin. J. Irrig. Drain. Eng. 111 (3), 265–275.
Hawkins, E.d., Sutton, R., 2011. The potential to narrow uncertainty in projections of regional precipitation change. Clim. Dyn. 37 (1), 407–418. https://doi.org/10.1007/s00382-010-0810-6.
Jeffrey, S.J., Carter, J.O., Moodie, K.B., Beswick, A.R., 2001. Using spatial interpolation to construct a comprehensive archive of Australian climate data. Environ. Modell. Software 16 (4), 309–330. https://doi.org/10.1016/S1364-8152(01)00008-1.
Jensen, M.E., Haise, H.R., 1963. Estimating evapotranspiration from solar radiation. Proc. Am. Soc. Civ. Eng., J. Irrig. Drain. Div. 89, 15–41.
Keenan, T.F., Luo, X., Zhang, Y., Zhou, S., 2020. Ecosystem aridity and atmospheric CO2. Science 368 (6488), 251. https://doi.org/10.1126/science.abb5449.
Kirono, D.G.C., Kent, D.M., Hennessy, K.J., Mpelasoka, F., 2011. Characteristics of Australian droughts under enhanced greenhouse conditions: results from 14 global climate models. J. Arid Environ. 75 (6), 566–575.
Kirono, D.G.C., Kent, D.M., 2011. Assessment of rainfall and potential evaporation from global climate models and its implications for Australian regional drought projection. Int. J. Climatol. 31 (9), 1295–1308. https://doi.org/10.1002/joc.2165.
Kumar, K.K., Kumar, K.R., Rakhecha, P.R., 1987. Comparison of Penman and Thornthwaite methods of estimating potential evapotranspiration for Indian conditions. Theor. Appl. Climatol. 38 (3), 140–146.
Labudová, L., Labuda, M., Takáč, J., 2017. Comparison of SPI and SPEI applicability for drought impact assessment on crop production in the Danubian Lowland and the East Slovakian Lowland. Theor. Appl. Climatol. 128 (1), 491–506. https://doi.org/10.1007/s00704-016-1870-2.
Liaw, A., Wiener, M., 2002. Classification and regression by randomForest. R. News 2 (3), 18–22.
Liu, D.L., Zuo, H., 2012. Statistical downscaling of daily climate variables for climate change impact assessment over New South Wales, Australia. Clim. Change 115 (3-4), 629–666. https://doi.org/10.1007/s10584-012-0464-y.
Lobell, D.B., Hammer, G.L., Chenu, K., Zheng, B., McLean, G., Chapman, S.C., 2015. The shifting influence of drought and heat stress for crops in northeast Australia. Glob. Change Biol. 21 (11), 4115–4127. https://doi.org/10.1111/gcb.13022.
Lu, J., Carbone, G.J., Grego, J.M., 2019. Uncertainty and hotspots in 21st century projections of agricultural drought from CMIP5 models. Sci. Rep. 9 (1), 4922. https://doi.org/10.1038/s41598-019-41196-z.
Luo, Q., Bellotti, W., Williams, M., Bryan, B., 2005. Potential impact of climate change on wheat yield in South Australia. Agric. For. Meteorol. 132 (3), 273–285. https://doi.org/10.1016/j.agrformet.2005.08.003.
Mckee, T.B., Doesken, N.J., Kleist, J., 1993. The relationship of drought frequency and duration to time scales. In: Proceedings of the 8th conference on applied climatology. American Meteorological Society, pp. 179–183.
Milly, P.C.D., Dunne, K.A., 2016. Potential evapotranspiration and continental drying. Nat. Clim. Change 6, 946. https://doi.org/10.1038/nclimate3046.
Mishra, A.K., Singh, V.P., 2010. A review of drought concepts. J. Hydrol. 391 (1-2), 202–216. https://doi.org/10.1016/j.jhydrol.2010.07.012.
Morim, J., Hemer, M., Wang, X.L., Cartwright, N., Trenham, C., Semedo, A., Young, I., Bricheno, L., Camus, P., Casas-Prat, M., Erikson, L.i., Mentaschi, L., Mori, N., Shimura, T., Timmermans, B., Aarnes, O., Breivik, Ø., Behrens, A., Dobrynin, M., Menendez, M., Staneva, J., Wehner, M., Wolf, J., Kamranzad, B., Webb, A., Stopa, J., Andutta, F., 2019. Robustness and uncertainties in global multivariate wind-wave climate projections. Nat. Clim. Change. 9 (9), 711–718. https://doi.org/10.1038/s41558-019-0542-5.
Naumann, G., Alfieri, L., Wyser, K., Mentaschi, L., Betts, R.A., Carrao, H., Spinoni, J., Vogt, J., Feyen, L., 2018. Global changes in drought conditions under different levels of warming. Geophys. Res. Lett. 45 (7), 3285–3296. https://doi.org/10.1002/2017gl076521.
Niemeyer, S., 2008. New drought indices. In: López-Francos, A. (Ed.), Drought management: scientific and technological innovations. Options Méditerranéennes : Série A. Séminaires Méditerranéens. CIHEAM, Zaragoza, pp. 267–274.
Parsons, D.J., Rey, D., Tanguy, M., Holman, I.P., 2019. Regional variations in the link between drought indices and reported agricultural impacts of drought. In: Agric. Syst. 173. pp. 119–129. https://doi.org/10.1016/j.agsy.2019.02.015.
Penman, H.L., 1948. Natural evaporation from open water, bare soil and grass. Proc. R. Soc. Lond. A 193 (1032), 120–145.
Potop, V., Možný, M., Soukup, J., 2012. Drought evolution at various time scales in the lowland regions and their impact on vegetable crops in the Czech Republic. Agric. For. Meteorol. 156, 121–133. https://doi.org/10.1016/j.agrformet.2012.01.002.
Pritchard, S.G., Rogers, H.H., Prior, S.A., Peterson, C.M., 1999. Elevated CO2 and plant structure: a review. Glob. Change Biol. 5 (7), 807–837. https://doi.org/10.1046/j.1365-2486.1999.00268.x.
Randall, D.A., et al., 2007. Climate Models and their Evaluation, Climate Change 2007: The Physical Science Basis. Contribution of Working Group I to the Fourth Assessment Report of the IPCC (FAR). Cambridge University Press, pp. 589–662.
Sheffield, J., Wood, E.F., Roderick, M.L., 2012. Little change in global drought over the past 60 years. Nature 491 (7424), 435–438.
Shi, L., Feng, P., Wang, B., Li Liu, D.e., Cleverly, J., Fang, Q., Yu, Q., 2020. Projecting potential evapotranspiration change and quantifying its uncertainty under future climate scenarios: a case study in southeastern Australia. J. Hydrol. 584, 124756. https://doi.org/10.1016/j.jhydrol.2020.124756.
Stagge, J.H., Tallaksen, L.M., Xu, C., Van Lanen, H., 2014. Standardized precipitation-evapotranspiration index (SPEI): Sensitivity to potential evapotranspiration model and parameters. In: Proceedings of FRIEND-water, pp. 367–373.
Stagge, J.H., Tallaksen, L.M., Gudmundsson, L., Van Loon, A.F., Stahl, K., 2015. Candidate Distributions for Climatological Drought Indices (SPI and SPEI): candidate distributions for climatological drought indices. Int. J. Climatol. 35 (13), 4027–4040. https://doi.org/10.1002/joc.4267.
Svoboda, M., Hayes, M., Wood, D., 2012. Standardized Precipitation Index User Guide. World Meteorological Organization Geneva, Switzerland.
Tabari, H., Kisi, O., Ezani, A., Hosseinzadeh Talaee, P., 2012. SVM, ANFIS, regression and climate based models for reference evapotranspiration modeling using limited climatic data in a semi-arid highland environment. J. Hydrol. 444-445, 78–89. https://doi.org/10.1016/j.jhydrol.2012.04.007.
Taylor, K.E., Stouffer, R.J., Meehl, G.A., 2012. An overview of cmip5 and the experiment design. Bull. Am. Meteorol. Soc. 93 (4), 485–498. https://doi.org/10.1175/bams-d-11-00094.1.
Thornthwaite, C.W., 1948. An approach toward a rational classification of climate. Geogr. Rev. 38 (1).
Touma, D., Ashfaq, M., Nayak, M.A., Kao, S.-C., Diffenbaugh, N.S., 2015. A multi-model and multi-index evaluation of drought characteristics in the 21st century. J. Hydrol. 526, 196–207. https://doi.org/10.1016/j.jhydrol.2014.12.011.
Tsakiris, G., Pangalou, D., Vangelis, H., 2007. regional drought assessment based on the Reconnaissance Drought Index (RDI). Water Resour. Manage. 21 (5), 821–833. https://doi.org/10.1007/s11269-006-9105-4.
Valipour, M., 2015. Temperature analysis of reference evapotranspiration models: reference evapotranspiration models. Met. Apps 22 (3), 385–394. https://doi.org/10.1002/met.1465.
van Dijk, A.I.J.M., et al., 2013. The Millennium Drought in southeast Australia (2001-2009): natural and human causes and implications for water resources, ecosystems, economy, and society: causes and impacts of Australia's record drought. Water Resour. Res. 49 (2), 1040–1057. https://doi.org/10.1002/wrcr.20123.
Vicente-Serrano, S.M., Beguería, S., López-Moreno, J.I., 2010. A multiscalar drought index sensitive to global warming: the standardized precipitation evapotranspiration index. J. Clim. 23 (7), 1696–1718. https://doi.org/10.1175/2009jcli2909.1.
Vicente-Serrano, S.M., Beguería, S., López-Moreno, J.I., 2011. Comment on "Characteristics and trends in various forms of the Palmer Drought Severity Index (PDSI) during 1900–2008" by Aiguo Dai. J. Geophys. Res. 116 (D19). https://doi.org/10.1029/2011JD016410.
Vicente-Serrano, S.M., McVicar, T.R., Miralles, D.G., Yang, Y., Tomas-Burguera, M., 2020. Unraveling the influence of atmospheric evaporative demand on drought and its response to climate change. WIREs Clim. Change 11 (2). https://doi.org/10.1002/wcc.v11.210.1002/wcc.632.
Vicente-Serrano, S.M., Van der Schrier, G., Beguería, S., Azorin-Molina, C., Lopez-Moreno, J.-I., 2015. Contribution of precipitation and reference evapotranspiration to drought indices under different climates. J. Hydrol. 526, 42–54. https://doi.org/10.1016/j.jhydrol.2014.11.025.
Wang, B., Chen, C., Liu, D.L., Asseng, S., Yu, Q., Yang, X., 2015. Effects of climate trends and variability on wheat yield variability in eastern Australia. Clim. Res. 64 (2), 173–186.
Wang, B., Liu, D.L., Waters, C., Yu, Q., 2018. Quantifying sources of uncertainty in projected wheat yield changes under climate change in eastern Australia. Clim. Change 151 (2), 259–273. https://doi.org/10.1007/s10584-018-2306-z.
Watson, J., Zheng, B., Chapman, S., Chenu, K., 2017. Projected impact of future climate on water-stress patterns across the Australian wheatbelt. J. Exp. Bot. 68 (21–22), 5907–5921. https://doi.org/10.1093/jxb/erx368.
Wong, G., Lambert, M.F., Leonard, M., Metcalfe, A.V., 2010. Drought analysis using trivariate copulas conditional on climatic states. J. Hydrol. Eng. 15 (2), 129–141. https://doi.org/10.1061/(ASCE)HE.1943-5584.0000169.
Yang, Y., et al., 2020. Comparing Palmer Drought Severity Index drought assessments using the traditional offline approach with direct climate model outputs. Hydrol. Earth Syst. Sci. 24 (6), 2921–2930. https://doi.org/10.5194/hess-24-2921-2020.
Yang, Y., Zhang, S., McVicar, T.R., Beck, H.E., Zhang, Y., Liu, B., 2018. Disconnection between trends of atmospheric drying and continental runoff. Water Resour. Res. 54 (7), 4700–4713. https://doi.org/10.1029/2018wr022593.
Yang, Y., Roderick, M.L., Zhang, S., McVicar, T.R., Donohue, R.J., 2019. Hydrologic implications of vegetation response to elevated CO2 in climate projections. Nat. Clim. Change 9 (1), 44–48. https://doi.org/10.1038/s41558-018-0361-0.
Yao, N., Li, Y., Li, L., Peng, L., Feng, H., 2019. Influence of the accuracy of reference crop evapotranspiration on drought monitoring using standardized precipitation evapotranspiration index in China. Land Degrad. Dev.(ja). https://doi.org/10.1002/ldr.3447.
Yip, S., Ferro, C.A.T., Stephenson, D.B., Hawkins, E.d., 2011. A simple, coherent framework for partitioning uncertainty in climate predictions. J. Climate 24 (17), 4634–4643. https://doi.org/10.1175/2011jcli4085.1.

Yu, M., Li, Q., Hayes, M.J., Svoboda, M.D., Heim, R.R., 2014. Are droughts becoming more frequent or severe in China based on the Standardized Precipitation Evapotranspiration Index: 1951–2010? Int. J. Climatol. 34 (3), 545–558. https://doi.org/10.1002/joc.3701.

Zhang, Y., Yu, Z., Niu, H., 2018. Standardized Precipitation Evapotranspiration Index is highly correlated with total water storage over China under future climate scenarios. Atmos. Environ. 194, 123–133. https://doi.org/10.1016/j.atmosenv.2018.09.028.

Zhao, T., Dai, A., 2015. The Magnitude and causes of global drought changes in the twenty-first century under a low-moderate emissions scenario. J. Clim. 28 (11), 4490–4512. https://doi.org/10.1175/JCLI-D-14-00363.1 %J Journal of Climate.

Zhao, T., Dai, A., 2017. Uncertainties in historical changes and future projections of drought. Part II: model-simulated historical and future drought changes. Clim. Change 144 (3), 535–548. https://doi.org/10.1007/s10584-016-1742-x.